Experimental Section

The FAB mass spectra were taken on a Kratos MS 50 mass spectrometer equipped with a magnet having a mass range of 10 000 Da at full (8-kV) accelerating voltage. The atom beam was provided with an Ion Tech FAB gun operating with xenon at 8 kV with a current of 30–40 μA. The magnet was typically scanned a rate of 100 s/decade.

Acknowledgment. We thank the SERC (UK) and Churchill College, Cambridge, for financial support.

Registry No. 1, 9007-92-5; **2**, 9007-43-6.

Stereochemically Constrained Peptides. Theoretical and Experimental Studies on the Conformations of Peptides Containing 1-Aminocyclohexanecarboxylic Acid

P. K. C. Paul,† M. Sukumar,† R. Bardi,‡ A. M. Piazzesi,‡ G. Valle,‡ C. Toniolo,‡ and P. Balaram*†

Contribution from the Molecular Biophysics Unit, Indian Institute of Science, Bangalore 560 012, India, and Biopolymer Research Centre, CNR, Department of Organic Chemistry, University of Padova, 35131, Padova, Italy. *Received March 27, 1986*

Abstract: Conformational energy calculations on the model system *N*-acetyl-1-aminocyclohexanecarboxylic acid *N'*-methylamide (Ac-Acc^6-NHMe), using an average geometry derived from 13 crystallographic observations, establish that the Acc^6 residue is constrained to adopt conformations in the $3_{10}/\alpha$-helical regions of ϕ, ψ space ($\phi = \pm 50 \pm 20°$, $\psi = \pm 50 \pm 20°$). In contrast, the α,α-dialkylated residue with linear hydrocarbon side chains, α,α-di-*n*-propylglycine favors fully extended backbone structures ($\phi \approx \psi \approx 180°$). The crystal structures of two model peptides, Boc-(Acc^6)$_3$-OMe (type III β-turn at -Acc^6(1)-Acc^6(2)-) and Boc-Pro-Acc^6-Ala-OMe (type II β-turn at -Pro-Acc^6-), establish that Acc^6 residues can occupy either position of type III β-turns and the $i + 2$ position of type II β-turns. The stereochemical rigidity of these peptides is demonstrated in solution by NMR studies, which establish the presence of one intramolecular hydrogen bond in each peptide in $CDCl_3$ and $(CD_3)_2SO$. Nuclear Overhauser effects permit characterization of the β-turn conformations in solution and establish their similarity to the solid-state structures. The implications for the use of Acc^6 residues in conformational design are considered.

The introduction of α,α-dialkylated amino acids into peptide chains provides a means of restricting the available range of backbone conformations.[1] The best studied member of this class of amino acids is α-aminoisobutyric acid (Aib).[2] The Aib residue (**1**) has been shown to strongly stabilize conformations in the $3_{10}/\alpha$-helical regions of the conformational map ($\phi \sim \pm 60 \pm 20°$, $\psi \sim \pm 30 \pm 20°$).[3] Peptides containing the residues α,α-diethylglycine (Deg; **2**) and α,α-di-*n*-propylglycine (Dpg; **3**) have been shown to occur in fully extended conformations ($\phi \sim 180°$, $\psi \sim 180°$).[4] Preliminary studies on fully protected peptides containing 1-aminocycloalkanecarboxylic acids (Acc^n, where n is the number of carbon atoms in the cycloalkane ring) suggest that both 1-aminocyclopentanecarboxylic acid (Acc^5, **4**)[5] and 1-aminocyclohexanecarboxylic acid (Acc^6, **5**) residues[6] stabilize folded conformations similar to those observed in Aib peptides. A synthetic chemotactic peptide analogue formyl-Met-Acc^6-Phe-OMe has been shown to possess significantly higher biological activity than the parent peptide, formyl-Met-Leu-Phe-OMe[7], stimulating interest in the conformational characteristics of Acc^6 residues. In this report we present conformational energy calculations on Ac-Acc^6-NHMe and compare the results obtained with similar computations for Aib[1a,8] and Dpg[4a,c] residues. An

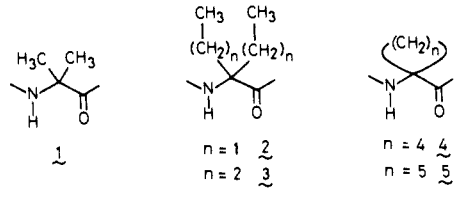

1

n = 1 **2**
n = 2 **3**

n = 4 **4**
n = 5 **5**

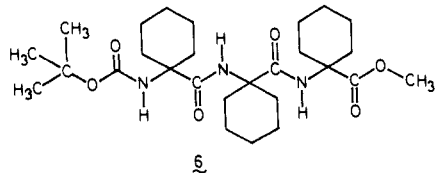

6

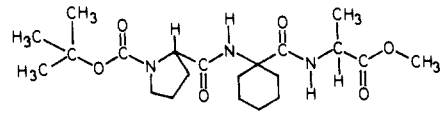

7

† Indian Institute of Science.
‡ University of Padova.

(1) (a) Marshall, G. R.; Bosshard, H. E. *Circ. Res., Suppl.* **1972**, *30* and *31*, 143–150. (b) Marshall, G. R.; Bosshard, H. E.; Kendrick, N. C. E.; Turk, J.; Balasubramanian, T. M.; Cobb, S. M. H.; Moore, M.; Leduc, L.; Needleman, P. In *Peptides: Proceedings of the Fourteenth European Peptide Symposium*; Loffet, A., Ed.; Editions de l'Universite de Bruxelles: Brussels, Belgium, 1972; pp 361–369.

(2) (a) Abbreviations used: Aib, α-aminoisobutyric acid; Acc^n, 1-aminocycloalkanecarboxylic acid with n atoms in the cycloalkane ring; Deg, α,α-diethylglycine; Dpg, α,α-di-*n*-propylglycine; Boc, *tert*-butyloxycarbonyl; Z, benzyloxycarbonyl; *p*BrBz, *p*-bromobenzoyl; *m*ClAc, monochloroacetyl; (b) All chiral amino acids used are of the L configuration. (c) Backbone torsion angles are defined according to the IUPAC–IUB Commission on Biochemical Nomenclature: *Biochemistry* **1970**, *9*, 3471–3479.

(3) For leading references see: (a) Prasad, B. V. V.; Balaram, P. *CRC Crit. Revs. Biochem.* **1984**, *16*, 307–348. (b) Toniolo, C.; Bonora, G. M.; Bavoso, A.; Benedetti, E.; Di Blasio, B.; Pavone, V.; Pedone, C. *Biopolymers* **1983**, *22*, 205–215. (c) Bosch, R.; Jung, G.; Schmitt, H.; Winter, W. *Biopolymers* **1985**, *24*, 979–999. (d) Smith, G. D.; Pletnev, V. Z.; Duax, W. L.; Balasubramanian, T. M.; Bosshard, H. E.; Czerwinski, E. W.; Kendrick, N. C. E.; Mathews, F. S.; Marshall, G. R. *J. Am. Chem. Soc.* **1981**, *103*, 1493–1501.

(4) (a) Benedetti, E.; Toniolo, C.; Hardy, P.; Barone, V.; Bavoso, A.; Di Blasio, B.; Grimaldi, P.; Lelj, F.; Pavone, V.; Pedone, C.; Bonora, G. M.; Lingham, I. *J. Am. Chem. Soc.* **1984**, *106*, 8146–8152. (b) Bonora, G. M.; Toniolo, C.; Di Blasio, B.; Pavone, V.; Pedone, C.; Benedetti, E.; Lingham, I.; Hardy, P. M. *J. Am. Chem. Soc.* **1984**, *106*, 8152–8156. (c) Barone, V.; Bavoso, A.; Di Blasio, B.; Grimaldi, P.; Lelj, F.; Pavone, V.; Pedone, C. *Biopolymers* **1985**, *24*, 1759–1767.

(5) Bardi, R.; Piazzesi, A. M.; Toniolo, C.; Sukumar, M.; Balaram, P. *Biopolymers*, in press.

(6) Bardi, R.; Piazzesi, A. M.; Toniolo, C.; Sukumar, M.; Raj, P. A.; Balaram, P. *Int. J. Pept. Protein Res.* **1985**, *25*, 628–639.

(7) Sukumar, M.; Raj, P. A.; Balaram, P.; Becker, E. L. *Biochem. Biophys. Res. Commun.* **1985**, *128*. 339–344.

0002-7863/86/1508-6363$01.50/0

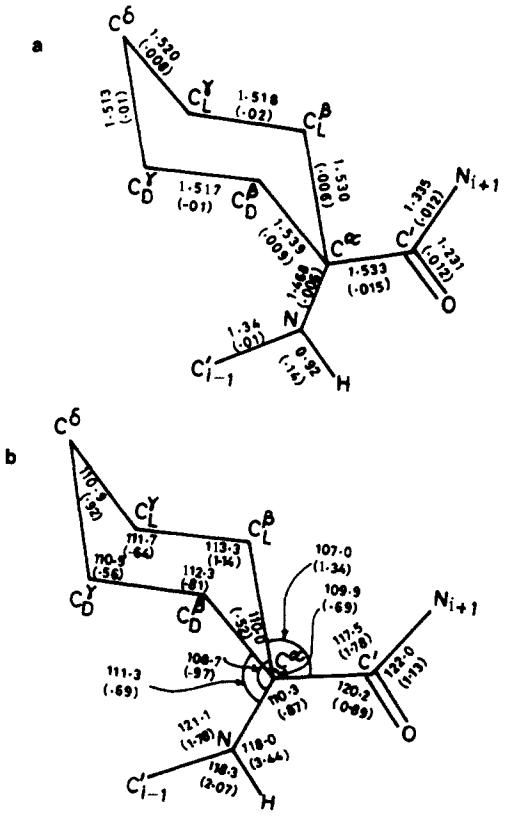

Figure 1. Average geometry of the Acc^6 residue derived from an analysis of crystal structures: (a) bond lengths (b) bond angles. Standard deviations are given in parentheses.

average geometry for the Acc^6 residue is derived from the results of several X-ray crystallographic determinations of the structures of Acc^6 derivatives and peptides. The occurrence of Acc^6 residues in β-turn conformations is exemplified by crystallographic and spectroscopic studies of two tripeptides, Boc-(Acc^6)$_3$-OMe (**6**) and Boc-Pro-Acc^6-Ala-OMe (**7**). The implications of the use of Acc^6 residues in conformationally constrained synthetic peptides are also considered.

Experimental Section

Conformational Energy Calculations. Geometry of the Acc^6 Residue. The average bond lengths and bond angles of the Acc^6 ring were derived from an analysis of the following crystal structures: Boc-Acc^6-OH,[9a] *p*BrBz-Acc^6-OH,[9a] Boc-(Acc^6)$_2$-OH,[9a] Boc-Met-Acc^6-OMe,[9a] Z-(Acc^6)$_2$O,[9a] *m*ClAc-Acc^6-OH,[9a] Boc-Aib-Acc^6-OMe,[6] Boc-Aib-Acc^6-NHMe,[6] Boc-(Acc^6)$_3$-OMe,[9b] and Boc-Pro-Acc^6-Ala-OMe.[9b] A total of 13 Acc^6 residues were used. The data analysis was carried out as described for the Aib residue by Paterson et al.[8c] The C$^\beta$ carbon atom in the Acc^6 residue that occupies the same position as C$^\beta$ in an L-amino acid is designated as C$^\beta_L$ and the other atom is C$^\beta_D$. Furthermore, the carbon atoms bonded to C$^\beta_L$ and C$^\beta_D$ are designated as C$^\gamma_L$ and C$^\gamma_D$, respectively. The results of the analysis are summarized in Figure 1. The details of the parameters obtained for individual crystal structures are listed in Table S-1 (supplementary material).

Energy Calculations. Conformational energies were calculated by using empirical potential energy functions and energy parameters described earlier.[10] The total conformational energy (V_{tot}) is the sum of the electrostatic energy (V_{es}), the nonbonded energy (V_{nb}), and the torsional strain energy (V_{tor}). V_{nb} was evaluated with the Buckingham "6-exp" potential, V_{es} was calculated with a monopole approximation, while a threefold potential was used in determining V_{tor}.[10] The residual charges on backbone atoms alone were considered, while those on the side chains were ignored. Conformational energies were calcualted at 10° intervals in the ϕ, ψ plane with use of a grid search procedure. A finer grid search at 2° intervals was performed in the low-energy regions to locate the conformations corresponding to a minimum. Conformational energy maps were computed for *N*-acetyl-Acc^6 *N'*-methylamide (Ac-Acc^6-NHMe) with both axial and equatorial orientations of the amino and carboxyl groups. Maps were also computed for Ac-Aib-NHMe[8c] and Ac-Dpg-NHMe,[4a] for comparison, using standard geometries.

Table I. Crystallographic Data for Boc-(Acc^6)$_3$-OMe (**6**) and Boc-Pro-Acc^6-Ala-OMe (**7**)

	6	**7**
molecular formula	$C_{27}H_{45}N_3O_6$	$C_{21}H_{35}N_3O_6$
M, amu	507.6	425.5
density (calcd), g cm^{-3}	1.14	1.16
density (exptl), g cm^{-3}	1.10	1.15
space group	$P2_1/n$	$P1$
Z	4	1
a, Å	15.066 (3)	10.760 (3)
b, Å	19.301 (3)	9.870 (3)
c, Å	10.293 (3)	6.003 (3)
α, Å		99.6 (1)
β, deg	97.3 (1)	103.3 (1)
γ, deg		92.2 (1)
reflections [$I \geq 3\sigma(I)$]	2383	1371
R value	0.073	0.066
R_w value	0.074	0.070

Synthesis of Peptides. Peptides **6** and **7** were prepared by conventional solution phase procedures with dicyclohexylcarbodiimide as a condensing agent. Representative procedures have been described earlier.[6] In the case of peptide **6**, coupling reactions were carried out at room temperature. Peptides **6** and **7** were purified by silica gel column chromatography with $CHCl_3$ and 1% MeOH–$CHCl_3$ as eluents. The peptides were obtained as white crystalline solids (**6**, mp 168–170 °C; **7**, mp 152–154 °C), homogeneous by TLC on silica gel (solvent, $CHCl_3$:MeOH (9:1): **6**, R_f 0.7; **7**, R_f 0.66). The peptides yielded 270-MHz ^{1}H NMR fully consistent with their structures.

X-ray Diffraction. Single crystals of **6** and **7** were grown from aqueous methanolic solutions. X-ray diffraction data were collected on a Phillips PW 1100 four-circle diffractometer with use of Mo Kα radiation, monochromatized by a graphite crystal (λ = 0.71069 Å). Intensities were corrected for Lorentz and polarization effects and put on an absolute scale. No absorption corrections were applied. The crystallographic data for peptides **6** and **7** are summarized in Table I. The structures were solved by application of the direct methods program MULTAN[11] and refined by conventional least-squares procedures, as described earlier.[6] In the case of **7**, disorder at the Pro residue was observed. Population parameters were applied to the C(8) and C(80) atoms. Refinement of positional and isotropic thermal parameters for these atoms resulted in a change of the thermal parameters to values close to those of the other carbon atoms. Sites C(8) and C(80) were refined with population parameters 0.60 and 0.40, respectively. Refinements were carried out by allowing all non-hydrogen atoms to vibrate anisotropically (except C(8) and C(80) in **7**), while hydrogen atoms were placed in calculated, idealized positions (C–H, N–H = 1.0 Å) but not varied. Calculations were carried out with the SHELX program.[12] The final conventional R values were 0.073 (R_w = 0.074) for **6** and 0.066 (R_w = 0.070) for **7**. The final positional parameters of the non-hydrogen atoms along with equivalent, isotropic thermal factors are listed in Tables II and III. Structure factor tables, anisotropic temperature factors, hydrogen positional parameters, and tables of bond lengths and bond angles for structures **6** and **7** are available as supplementary material.

NMR Studies. ^{1}H NMR spectra were recorded on a Varian FT-80A spectrometer and on a Bruker WH-270 FT–NMR spectrometer at the Sophisticated Instruments Facility, Indian Institute of Science, Bangalore. All chemical shifts are expressed as δ (ppm) downfield from internal tetramethylsilane. Delineation of hydrogen-bonded NH groups was accomplished by using temperature and solvent dependence of NH chemical shifts and broadening of NH resonances by the free radical 2,2,6,6-tetramethylpiperidine-1-oxyl (Tempo), as described earlier.[6,13] NOE experiments were carried out at 270 MHz, at a probe temperature

(8) (a) Burgess, A. W.; Leach, S. J. *Biopolymers* **1973**, *12*, 2599–2605. (b) Pletnev, V. Z.; Gromov, E. P.; Popov, E. M. *Khim. Prir. Soedin.* **1973**, *9*, 224–229. (c) Paterson, Y.; Rumsey, S. M.; Benedetti, E.; Nemethy, G.; Scheraga, H. A. *J. Am. Chem. Soc.* **1981**, *103*, 2947–2955.

(9) (a) Valle, G.; Crisma, M.; Toniolo, C.; Sen, N.; Sukumar, M.; Balaram, P., manuscript in preparation. (b) This paper.

(10) Ramachandran, G. N.; Sasisekharan, V. *Adv. Protein Chem.* **1968**, *23*, 283–468.

(11) Main, P.; Fiske, S. J.; Hull, S. E.; Lessinger, L.; Germain, G.; Declercq, J. P.; Woolfson, M. M.: MULTAN 80. A System of Computer Programs for the Automatic Solution of Crystal Structures from X-Ray Diffraction Data, University of York, England and Louvain, Belgium, 1980.

(12) Sheldrick, G. M. SHELX-76. Program for Crystal Structure Determination, University of Cambridge, England, 1976.

(13) (a) Iqbal, M.; Balaram, P. *J. Am. Chem. Soc.* **1981**, *103*, 5548–5552. (b) Vijayakumar, E. K. S.; Balaram, P. *Biopolymers* **1983**, *22*, 2133–2140.

Table II. Fractional Coordinates (×10⁴) and Equivalent Isotropic Temperature Factors (Å², ×10³) for Boc-(-Acc⁶-)₃-OMe (**6**)[a]

atom	x	y	z	U_{eq}
O(1)	3218 (2)	1367 (2)	11697 (3)	73 (2)
O(2)	2368 (2)	1167 (2)	9756 (3)	81 (2)
O(3)	2339 (2)	2111 (2)	6703 (3)	75 (2)
O(4)	-166 (2)	2480 (2)	6910 (3)	71 (2)
O(5)	-1587 (2)	1276 (2)	7026 (4)	120 (3)
O(6)	-987 (2)	1694 (2)	8958 (4)	94 (3)
N(1)	3514 (2)	1933 (2)	9931 (3)	58 (2)
N(2)	2068 (2)	2606 (2)	8602 (4)	56 (2)
N(3)	648 (2)	1680 (2)	8103 (3)	50 (2)
C(1)	1774 (5)	1080 (6)	12370 (9)	139 (7)
C(2)	3224 (7)	957 (6)	13821 (6)	139 (7)
C(3)	2848 (8)	156 (4)	11909 (9)	140 (7)
C(4)	2744 (4)	871 (3)	12425 (5)	84 (3)
C(5)	2999 (3)	1470 (3)	10408 (5)	61 (3)
C(6)	3516 (3)	2026 (3)	8525 (4)	60 (3)
C(7)	4142 (3)	2634 (3)	8316 (5)	84 (3)
C(8)	5130 (4)	2456 (5)	8705 (5)	119 (5)
C(9)	5384 (5)	1801 (6)	8038 (9)	162 (7)
C(10)	4793 (5)	1205 (5)	8335 (8)	132 (6)
C(11)	3809 (3)	1374 (4)	7868 (6)	89 (4)
C(12)	2571 (3)	2244 (3)	7859 (5)	57 (3)
C(13)	1181 (3)	2889 (2)	8133 (4)	58 (3)
C(14)	1224 (4)	3423 (3)	7035 (6)	81 (4)
C(15)	1735 (5)	4057 (4)	7494 (8)	123 (5)
C(16)	1320 (7)	4400 (4)	8613 (9)	141 (7)
C(17)	1310 (5)	3898 (4)	9744 (8)	116 (5)
C(18)	821 (4)	3240 (3)	9297 (5)	80 (4)
C(19)	521 (3)	2323 (2)	7649 (4)	52 (3)
C(20)	-1 (3)	1137 (2)	7674 (4)	53 (3)
C(21)	49 (3)	943 (3)	6237 (5)	71 (3)
C(22)	903 (4)	564 (3)	6067 (6)	93 (4)
C(23)	974 (4)	-96 (3)	6871 (7)	109 (5)
C(24)	967 (4)	79 (3)	8303 (7)	100 (4)
C(25)	172 (4)	500 (3)	8532 (5)	79 (4)
C(26)	-940 (3)	1386 (3)	7810 (6)	76 (3)
C(27)	-1860 (5)	1928 (7)	9185 (14)	151 (8)

[a] esd's are given in parentheses.

of 293 K, with a peptide concentration of 0.05 M. Undegassed samples were used in the NOE experiments. Difference NOE spectra[14] were obtained by sequential recording of perturbed and normal spectra (8K memory each) with low-power on-resonance saturation of a peak and by off-resonance shifting of the irradiation frequency, respectively. A delay time of 3.0 s was used between transients. The difference free induction decay was multiplied by a decaying exponential, prior to Fourier transformation.

Results and Discussion

Average Geometry and Theoretical Calculations. The average geometry derived for the Acc⁶ residue from an analysis of available crystal structures is summarized in Figure 1. The bond angles at the C^{α} atom of the Acc⁶ residue show deviations from tetrahedral values, which are similar to those observed for the Aib residue.[8c] An asymmetric geometry similar to Aib is obtained. The mean endocyclic torsion angle of ±54.6° is consistent with an almost perfect chair conformation, for the cyclohexane side chain in the Acc⁶ residue.[15] In almost all crystal structures containing Acc⁶, described so far,[6,9] the amino group occupies the axial position, in accordance with early expectations.[16] The only exception is the crystal structure of the free amino acid (H-Acc⁶-OH), where the carboxyl group occupies an axial position.[9a] Interestingly, the amino group occupies the axial position in the structure of the amino acid hydrochloride (H-Acc⁶-OH·HCl).[17]

Conformational energy maps have been computed for Ac-Acc⁶-NHMe with both axial and equatorial orientations of the amino group. The results are shown in Figure 2. Energy maps for Ac-Aib-NHMe and Ac-Dpg-NHMe using identical procedures are shown for comparison in Figure 3. Several noteworthy features emerge from these results.

In the Acc⁶ (-NH- axial) case the deepest energy minima lie in the right- and left-handed $\alpha/3_{10}$-helical region (region I) of ϕ, ψ space. A minimum is also observed for a quasiextended conformation (region II, $\phi = \pm 60°$, $\psi \sim 180°$). There is also a limited region (region III) of energetically accessible conformations corresponding to C_7 structures (3 >1 hydrogen bonded). For the Acc⁶ (-NH- equatorial) case region II shoots up in energy (~25 kcal mol⁻¹ above the minimum), while a new quasiextended structure is stabilized (region II′, $\phi \sim 180°$, $\psi \sim \pm 60°$). It is clear that 1,3-diaxial interactions between the axial substitutent and the axial $C^{\gamma}H$ groups determine the preference for the quasiextended region. Regions with $\phi \sim 180°$ are strongly disallowed when the -NH- group is axial, while the $\psi \sim 180°$ regions are extremely high in energy for the -CO- axial case. The lowest energy conformations occur at the grid points $\phi = \pm 52°$, $\psi = \pm 46°$ (-NH- axial) and $\phi = \pm 48°$, $\psi \sim \pm 60°$ (-NH- equatorial). The -NH- axial minimum is ~1.6 kcal mol⁻¹ lower in energy than the -NH- equatorial minimum. Perspective views of the low-energy conformations of Ac-Acc⁶-NHMe are shown in Figure 4.

In the case of Ac-Aib-NHMe (Figure 3a) energetically accessible conformations are observed in the α-helical ($\phi \sim \pm 55°$, $\psi \sim \pm 45°$), C_7 ($\phi \sim \pm 70°$, $\psi \sim \mp 70°$), fully extended ($\phi \sim 180°$, $\psi \sim 180°$), and quasiextended ($\phi \sim 180°$, $\psi \sim \pm 60°$ or $\phi \sim \pm 60°$, $\psi \sim 180°$) regions. The lowest energy conformation is observed at $\phi \sim \pm 50°$, $\psi \sim \pm 48°$. These observations are in complete agreement with earlier reports.[8]

The conformational energy map for Ac-Dpg-NHMe (Figure 3b) shows energy minima in the helical, fully extended, and quaisextended regions. The lowest energy conformation occurs in the fully extended region ($\phi \sim 180°$, $\psi \sim 180°$) and is about 3 kcal mol⁻¹ lower than the minimum in the helical region. In Ac-Dpg-NHMe, 81 side chain conformations are possible for each

Table III. Fractional Coordinates (×10⁴), Population Parameters (pp), and Equivalent Isotropic Temperature Factors (Å², ×10³) for Boc-L-Pro-Acc⁶-L-Ala-OMe (**7**)[a]

atom	pp	x	y	z	U_{eq}/U^*
O(1)	1.0	3894	8620	316	79 (3)
O(2)	1.0	1825 (5)	7960 (6)	130 (9)	65 (3)
O(3)	1.0	2052 (6)	4990 (7)	1877 (8)	73 (3)
O(4)	1.0	-916 (6)	5236 (6)	4391 (8)	61 (3)
O(5)	1.0	-2618 (6)	7716 (8)	3463 (9)	84 (4)
O(6)	1.0	-1603 (5)	8076 (6)	7222 (8)	62 (3)
N(1)	1.0	3158 (6)	6460 (7)	-1020 (12)	63 (3)
N(2)	1.0	180 (5)	4833 (6)	-895 (9)	41 (3)
N(3)	1.0	-260 (6)	6829 (6)	2579 (10)	55 (3)
C(1)	1.0	2857 (12)	10789 (12)	530 (23)	103 (9)
C(2)	1.0	5231 (11)	10607 (13)	1599 (23)	103 (8)
C(3)	1.0	3881 (14)	9887 (17)	4104 (18)	128 (9)
C(4)	1.0	3927 (9)	10019 (9)	1655 (15)	71 (5)
C(5)	1.0	2866 (7)	7702 (8)	-156 (11)	51 (4)
C(6)	1.0	2160 (7)	5334 (8)	-1964 (12)	51 (4)
C(7)	1.0	2896 (9)	4102 (9)	-2665 (16)	73 (5)
C(8)	0.6	4225 (20)	4385 (21)	-1133 (34)	104 (5)*
C(80)	0.4	4075 (20)	4829 (23)	-3368 (38)	74 (6)*
C(9)	1.0	4415 (10)	6059 (13)	-1275 (28)	135 (9)
C(10)	1.0	1469 (7)	5035 (7)	-75 (12)	50 (4)
C(11)	1.0	-676 (7)	4422 (7)	512 (11)	44 (3)
C(12)	1.0	-371 (8)	3022 (8)	1218 (12)	64 (4)
C(13)	1.0	-640 (9)	1860 (8)	-876 (14)	64 (4)
C(14)	1.0	-2028 (9)	1778 (9)	-2241 (15)	72 (5)
C(15)	1.0	-2386 (8)	3150 (8)	-2966 (13)	60 (4)
C(16)	1.0	-2050 (7)	4338 (7)	-923 (12)	50 (4)
C(17)	1.0	-563 (7)	5532 (8)	2680 (11)	46 (4)
C(18)	1.0	-307 (8)	7919 (8)	4527 (12)	51 (4)
C(19)	1.0	4 (11)	9316 (9)	3938 (18)	89 (7)
C(20)	1.0	-1671 (7)	7863 (7)	4892 (11)	51 (4)
C(21)	1.0	-2863 (9)	8077 (11)	7715 (16)	76 (6)

[a] esd's are given in parentheses.

(14) Rao, B. N. N.; Kumar, A.; Balaram, H.; Ravi, A.; Balaram, P. *J. Am. Chem. Soc.* **1983**, *105*, 7423–7428.
(15) Bixon, M.; Lifson, S. *Tetrahedron* **1967**, *23*, 769–784.
(16) Kenner, G. W.; Preston, J.; Sheppard, R. C. *J. Chem. Soc.* **1965**, 6239–6244.
(17) Chacko, K. K.; Srinivasan, R.; Zand, R. *J. Cryst. Mol. Struct.* **1971**, *1*, 261–269.

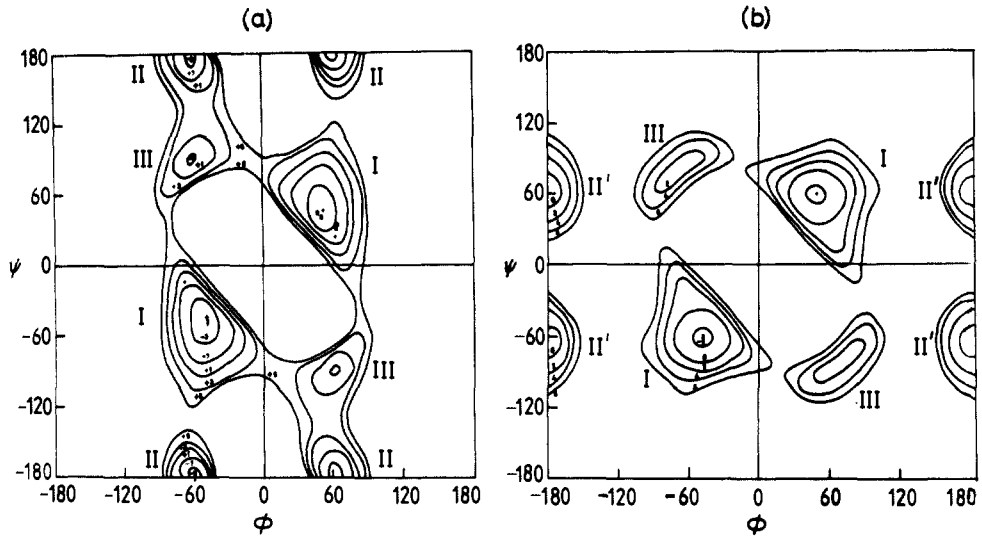

Figure 2. Conformational energy maps for Ac-Acc^6-NHMe: (a) -NH- axial, (b) -NH- equatorial. The lowest energy conformations are indicated (×) and the energy contours are drawn in steps of 2 kcal mol^{-1}. The crystallographically observed ϕ, ψ values (●) in Boc-Met-Acc^6-OMe, Boc-Aib-Acc^6-OMe, Boc-Aib-Acc^6-NHMe, Boc-(Acc^6)$_3$-OMe, and Boc-Pro-Acc^6-Ala-OMe are indicated.

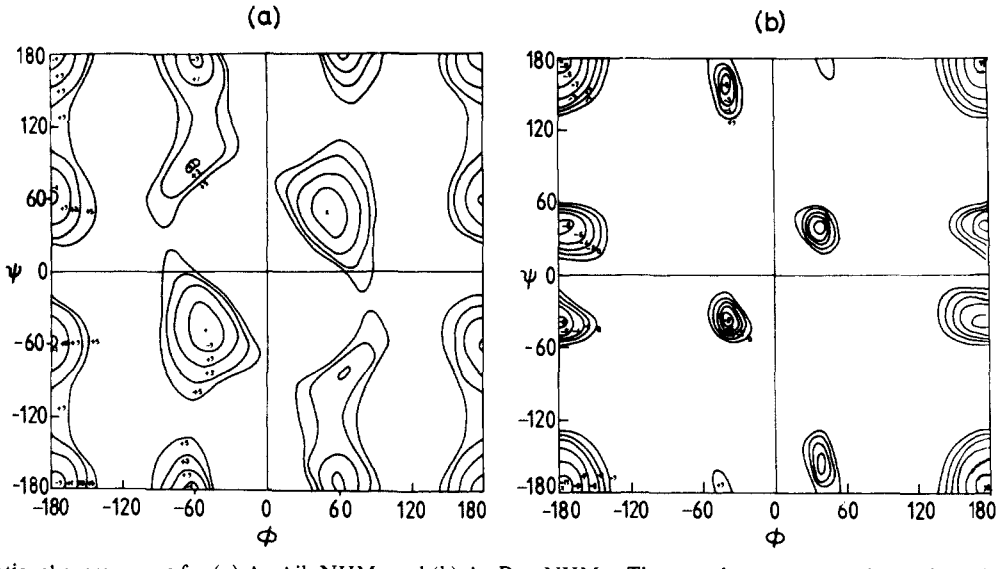

Figure 3. Conformational energy maps for (a) Ac-Aib-NHMe and (b) Ac-Dpg-NHMe. The map shown corresponds to side chain conformations χ_1, χ_2 of 60°, 180° and −60°, 180° for the L and D side chains, respectively.

ϕ, ψ value considering the gauche$^+$ (g$^+$), gauche$^-$ (g$^-$), and trans (t) rotamers about the C$^\alpha$–C$^\beta$ and C$^\beta$–C$^\gamma$ bonds of both *n*-propyl groups. Of these only the 9 symmetric cases were considered. The results establish that the g$^-$g$^-$, g$^-$t, g$^-$g$^+$, tg$^-$, tt, and tg$^+$ (for the *pro-S* substituent) are energetically very unfavorable due to side chain–side chain short contacts. Further the g$^+$g$^+$ (*pro-S*) conformation is completely disallowed by side chain–backbone contacts in the entire ϕ–ψ plane. Of the remaining two, g$^+$t (*pro-S*) has better energies at all regions of ϕ, ψ space as compared to g$^+$g$^-$ (*pro-S*), and this energy map is shown in Figure 3b. The results are in general agreement with those obtained by an energy minimization procedure, with the exception that the g$^+$g$^-$ conformations were favored in the fully extended regions, in the earlier study.[4a] It may be noted that only g$^+$t (g$^-$t) conformations have indeed been observed in the crystal structures of Dpg peptides, so far.[4a] A comparison of the maps in Figures 2 and 3 suggests that the Acc^6 residue is largely compelled to adopt conformations in the α-helical region with fully extended structures being completely ruled out. In contrast such conformations are indeed *highly likely* for Dpg residues, an expectation[4a,c] which has received some experimental support.[4b] For Aib, conformations in the $3_{10}/\alpha$-helical regions are favored, as already been borne out in extensive investigations.[3] However, the occasional observation of Aib in extended (quasi or fully) and C_7 regions in crystal structures[3a]

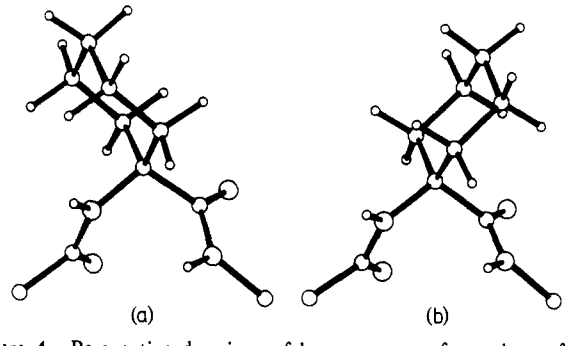

Figure 4. Perspective drawings of low-energy conformations of Ac-Acc^6-NHMe: (a) -NH- axial $\phi = -52°$, $\psi = -46°$, (b) -NH-equatorial $\phi = -48°$, $\psi = -60°$.

is in agreement with conformational energy calculations.

In order to provide experimental support for the conformational energy calculations summarized above, we describe structural studies on two Acc^6 containing protected tripeptides, Boc-(Acc^6)$_3$-OMe (**6**) and Boc-Pro-Acc^6-Ala-OMe (**7**).

Crystal Structures of Peptides 6 and 7. The molecular conformations of peptides **6** and **7**, determined in the solid state by X-ray diffraction, are shown in Figures 5 and 6, while the mo-

Table IV. Backbone Torsional Angles (deg)[a] in Peptides **6** and **7**

Boc-$(Acc^6)_3$-OMe (**6**)			Boc-Pro-Acc^6-Ala-OMe (**7**)		
$\omega_{Acc^6(1)}$	O(1)-C(5)-N(1)-C(6)	-167.5 (4)	ω_{Pro}	O(1)-C(5)-N(1)-C(6)	-171.5 (7)
$\phi_{Acc^6(1)}$	C(5)-N(1)-C(6)-C(12)	60.8 (6)	ϕ_{Pro}	C(5)-N(1)-C(6)-C(10)	-60.1 (9)
$\psi_{Acc^6(1)}$	N(1)-C(6)-C(12)-N(2)	29.5 (6)	ψ_{Pro}	N(1)-C(6)-C(10)-N(2)	136.6 (7)
$\omega_{Acc^6(2)}$	C(6)-C(12)-N(2)-C(13)	176.6 (4)	ω_{Acc^6}	C(6)-C(10)-N(2)-C(11)	174.9 (6)
$\phi_{Acc^6(2)}$	C(12)-N(2)-C(13)-C(19)	60.5 (6)	ϕ_{Acc^6}	C(10)-N(2)-C(11)-C(17)	61.5 (9)
$\psi_{Acc^6(2)}$	N(2)-C(13)-C(19)-N(3)	24.9 (6)	ψ_{Acc^6}	N(2)-C(11)-C(17)-N(3)	29.1 (9)
$\omega_{Acc^6(3)}$	C(13)-C(19)-N(3)-C(20)	178.0 (4)	ω_{Ala}	C(11)-C(17)-N(3)-C(18)	172.3 (7)
$\phi_{Acc^3(3)}$	C(19)-N(3)-C(20)-C(26)	-49.6 (5)	ϕ_{Ala}	C(17)-N(3)-C(18)-C(20)	-58.2 (9)
$\psi_{Acc^6(3)}$	N(3)-C(20)-C(26)-O(6)	-45.8 (6)	ψ_{Ala}	N(3)-C(18)-C(20)-O(6)	139.3 (6)

[a] esd's are given in parentheses. Torsion angles are given for one enantiomeric molecule.

Table V. Geometry of Hydrogen Bonds in the Crystals of **6** and **7**

donor D-H	acceptor A	symmetry equivalence of A	distances (Å) D---A	distances (Å) H---A	angle (deg) D—H---A
		Boc-$(Acc^6)_3$-OMe (**6**)			
N(3)-H	O(2)	x,y,z	3.076 (5)	2.091 (5)	167.8 (4)
N(1)-H	O(4)	$^1/_2 + x, ^1/_2 - y, ^1/_2 + z$	2.890 (5)	1.924 (5)	161.1 (4)
		Boc-Pro-Acc^6-Ala-OMe (**7**)			
N(3)-H	O(2)	x,y,z	3.21 (1)	2.38 (1)	140.1 (6)
N(2)-H	O(4)	$x,y,z-1$	2.90 (1)	1.90 (1)	179.5 (7)

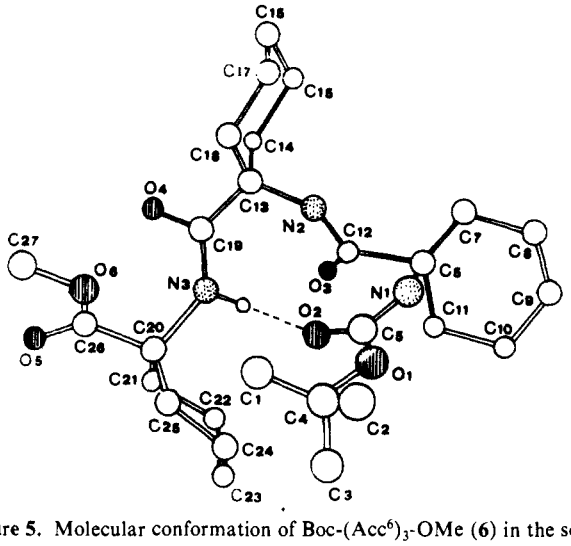

Figure 5. Molecular conformation of Boc-$(Acc^6)_3$-OMe (**6**) in the solid state.

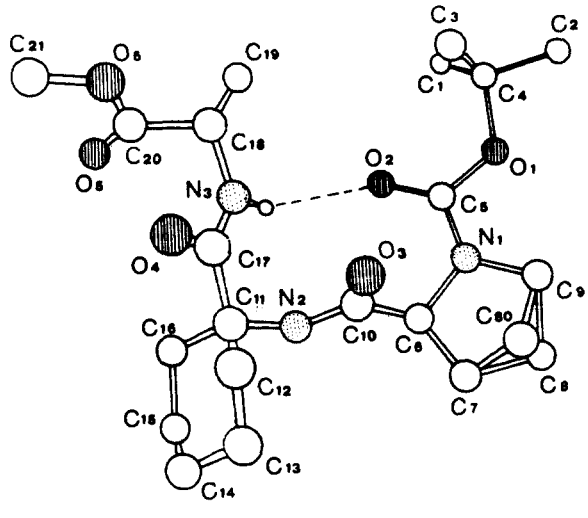

Figure 6. Molecular conformation of Boc-Pro-Acc^6-Ala-OMe (**7**) in the solid state. Note that C^γ Pro occupies two distinct positions.

lecular packing in the crystals is illustrated in Figures 7 and 8, respectively. The relevant backbone torsion angles[2] are listed in

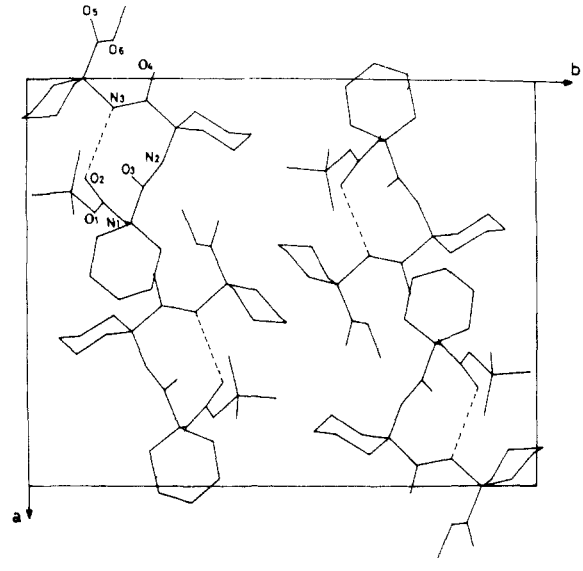

Figure 7. Molecular packing in crystals of Boc-$(Acc^6)_3$-OMe (**6**) viewed down the c axis.

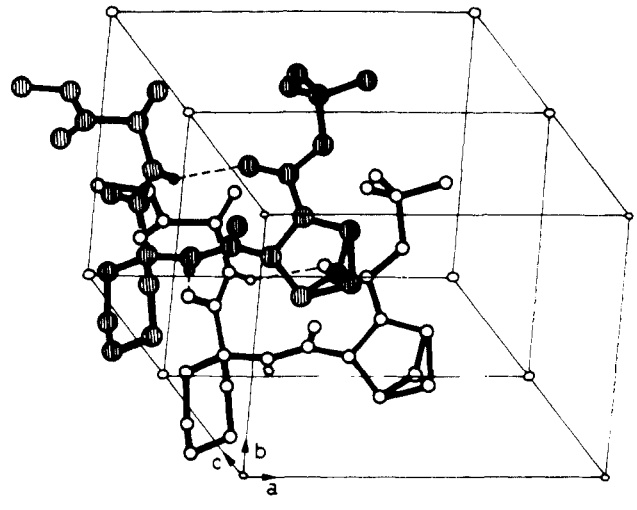

Figure 8. Molecular packing in crystals of Boc-Pro-Acc^6-Ala-OMe (**7**). Note that there is only one molecule per unit cell.

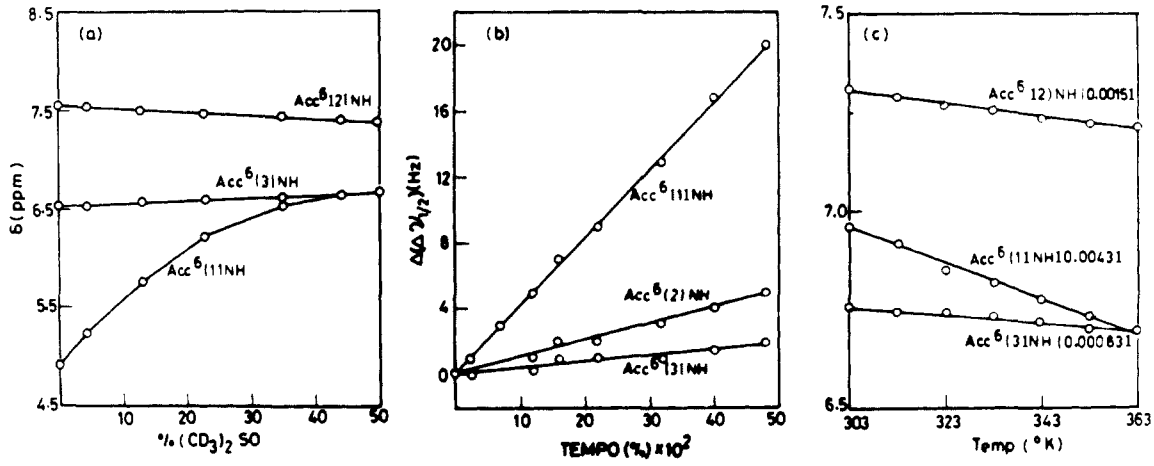

Figure 9. (a) Solvent dependence of NH chemical shifts in Boc-(Acc^6)$_3$-OMe (6) in $CDCl_3$–$(CD_3)_2SO$ mixtures. (b) Effect of Tempo on the line width of NH resonances in 6 in $CDCl_3$. $\Delta(\Delta\nu_{1/2})$ is the line broadening. (c) Temperature dependence of NH chemical shifts in $(CD_3)_2SO$ for 6. Temperature coefficients ($d\delta/dT$) are indicated in parentheses. Peptide concentration in all experiments is ~0.025 M.

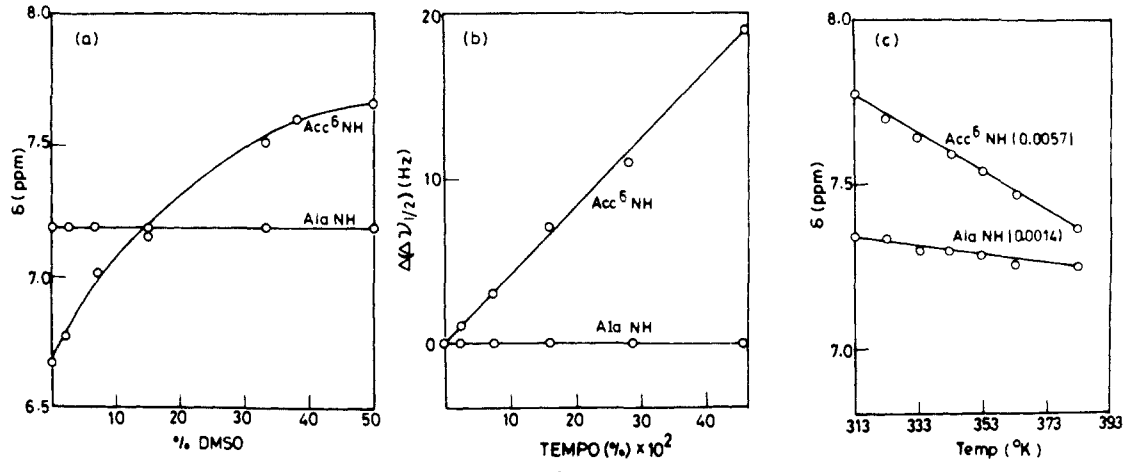

Figure 10. (a) Solvent dependence of NH chemical shifts in Boc-Pro-Acc^6-Ala-OMe (7) in $CDCl_3$–$(CD_3)_2SO$ mixtures. (b) Effect of Tempo on the line width of NH resonance in 7 in $CDCl_3$. $\Delta(\Delta\nu_{1/2})$ is the line broadening. (c) Temperature dependence of NH chemical shifts in $(CD_3)_2SO$ for 7. $d\delta/dT$ values are indicated in parentheses. Peptides concentrations in all experiments is ~0.025 M.

Table IV. The hydrogen bond parameters are given in Table V. The bond lengths and bond angles are largely unexceptional.

Peptide 6 adopts an almost ideal type III (III′) β-turn conformation[18,19] with Acc^6(1) (ϕ = ±60.8°, ψ = ±29.5°) and Acc^6(2) (ϕ = ±60.5, ψ = ±24.9°) as the i + 1 and i + 2 residues, respectively. The 4→1 intramolecular hydrogen bond (Boc CO---Acc^6(3)NH) has an N---O distance of 3.076 Å which is in the range expected for intramolecular hydrogen bonds in peptides.[20] The third Acc^6 residue also adopts a conformation in the helical region but has a handedness opposite to that of the preceding residue. This feature has been consistently observed in crystal structures of Aib containing oligopeptides.[3a] The mean endocyclic torsion angles for the cyclohexane rings of the three Acc^6 residues are Acc^6(1) 55.6 (8)°, Acc^6(2) 55.4 (8)°, and Acc^6(3) 54.0 (7)°. These values are very close to the expected torsion angles of 54.7° in cyclohexane, with a C–C–C bond angle of 111.5°.[15] A single intermolecular hydrogen bond between the Acc^6(1) NH group and Acc^6(2) CO groups of symmetry related molecules (N---O, 2.890 (5) Å) is observed in the crystal structure (Table V, Figure 7).

Peptide 7 adopts a type II β-turn conformation with Pro (ϕ = −60.1°, ψ = 136.6°) and Acc^6 (ϕ = 61.5°, ψ = 29.1°) as the i + 1 and i + 2 residues. A single *intramolecular* hydrogen bond is observed between the Boc CO and Ala NH groups (Figure 6). The N---O distance of 3.21 Å is at the upper limit of the range of values reported in a large number of peptide structures.[20] The ϕ, ψ values for Acc^6 deviate by ~20–30° from those expected in an ideal type II β-turn and result in a lengthening of the N---O distance. The Acc^6 residue again adopts a conformation in the left-handed $3_{10}/\alpha$-helical region of the ϕ, ψ map. The cyclohexane ring in 7 has a mean endocyclic torsion angle of 53.7 (4)°, which is representative of an almost ideal chair conformation. The pyrrolidine ring of Pro adopts two distinct conformations, with different occupancies. These are the C^{γ}_{exo} (C(8)) and C^{γ}_{endo} (C(80)) conformations, the ring having an approximate C_s (envelope) symmetry.[21] A single intermolecular hydrogen bond between the Acc^6 NH and Acc^6 CO groups of symmetry related molecules (N---O, 2.90 Å) stabilizes the crystal structure (Table V, Figure 8).

All four Acc^6 residues observed in the crystal structures of peptides 6 and 7 adopt backbone conformations in the $3_{10}/\alpha$-helical regions of ϕ, ψ space. Thus all Acc^6 residue conformations determined by X-ray diffraction fall into these regions (Figure 2a)

(18) (a) Venkatachalam, C. M. *Biopolymers* **1968**, *6*, 1425–1436. (b) Rose, G. D.; Gierasch, L. M.; Smith, J. A. *Adv. Protein Chem.* **1985**, *37*, 1–109.

(19) The conformational angles in ideal β-turns are as follows: type I, ϕ_{i+1} = −60°, ψ_{i+1} = −30°, ϕ_{i+2} = −90°, ψ_{i+2} = 0°; type II, ϕ_{i+1} = −60°, ψ_{i+1} = 120°, ϕ_{i+2} = 80°, ψ_{i+2} = 0°; type III, ϕ_{i+1} = −60°, ψ_{i+1} = −30°, ϕ_{i+2} = −60°, ψ_{i+2} = −30°. The enantiomeric type I′, II′, and III′ β-turns are obtained by inverting the signs of all torsion angles.

(20) (a) Karle, I. L. *The Peptides*; Gross, E., Meienhofer, J., Eds.; Academic Press: New York, 1981; Volume IV, pp 1–53. (b) Taylor, R.; Kennard, O.; Versichel, W. *Acta Crystallogr.* **1984**, *B40*, 280–288.

(21) (a) Ramachandran, G. N.; Lakshminarayanan, A. V.; Balasubramanian, R.; Tegoni, G. *Biochim. Biophys. Acta* **1970**, *221*, 165–181. (b) Ashida, T.; Kakudo, M. *Bull. Chem. Soc. Jpn.* **1974**, *47* 1129–1133.

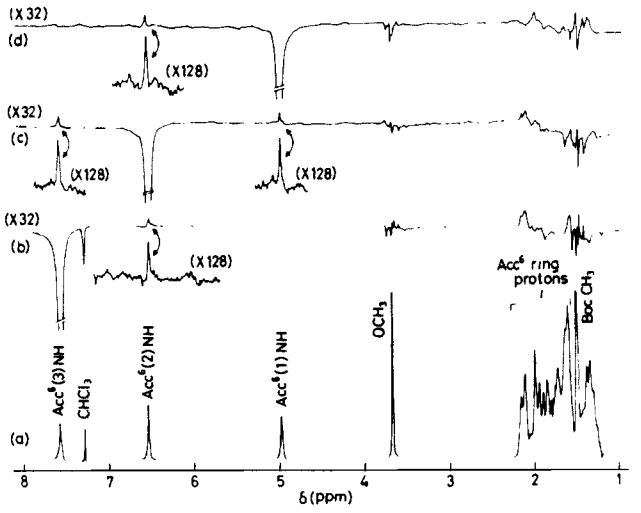

Figure 11. (a) 270-MHz ^{1}H NMR spectrum of Boc-(Acc^6)$_3$-OMe (**6**) in $CDCl_3$. (b–d) Difference NOE spectra obtained by irradiation of NH resonances: (b) Acc^6(3) NH, (c) Acc^6(2) NH, (d) Acc^6(1) NH. Vertical scale expansions are indicated against the traces. The difference spectra were recorded as described earlier,[14] using 1024 accumulations for both on and off resonance experiments, in each case. Peptide concentration ~0.05 M.

providing overwhelming support for the theoretical predictions. The results also experimentally establish that Acc^6 residues can occur at either position (i + 1, i + 2) of type III β-turns or at the i + 2 position of type II β-turns. These observations are relevant when employing Acc^6 residues to generate folded oligopeptide models.

NMR Studies. ^{1}H NMR studies were carried out in order to determine whether the folded structures, determined for **6** and **7** in the solid state, are maintained in solution. The delineation of solvent inaccessible or intramolecularly hydrogen bonded NH groups was carried out with use of temperature and solvent dependence of NH chemical shifts and free radical induced line broadening of NH resonances.[22] The results of these experiments are summarized in Figures 9 and 10 for peptides **6** and **7**, respectively. The assignments of NH resonances are trivial in **7**. In **6**, the upfield NH resonance in $CDCl_3$ is assigned to the Acc^6(1) NH (urethane) in $CDCl_3$.[13] The Acc^6(2) NH and Acc^6(3) NH resonances can be unambiguously identified by NOE experiments as described later. In peptide **6** the Acc^6(2) and Acc^6(3) NH groups display behavior characteristic of solvent shielded protons (relative insensitivity of chemical shifts to solvent composition in $CDCl_3$–$(CD_3)_2SO$ mixtures, insensitivity of line widths to the presence of the free radical 2,2,6,6-tetramethylpiperidine-1-oxyl (Tempo), and low $d\delta/dT$ values (<0.003 ppm/K) in $(CD_3)_2SO$.[22] The Acc^6(1) NH is clearly solvent exposed (Figure 9). These results are consistent with a β-turn conformations for **6**, in which Acc^6(3) NH is involved in an intramolecular 4→1 hydrogen bond with the Boc CO group, while Acc^6(2) NH is sterically shielded from the solvent by the flanking cyclohexyl groups. Nuclear Overhauser effect (NOE) studies[14,23] illustrated in Figure 11 and summarized in Table VI permit determination of the nature of the β-turn[14] and assignment of the NH resonances to specific Acc^6 residues. Irradiation of the Acc^6(1) NH results in an enhancement of ~1.9% of the resonance at δ 6.53, which may then be assigned to the Acc^6(2) NH group. There are no β-turn or other regular, sterically allowed conformations which bring the N_iH and $N_{i+2}H$ protons to distances <3.0 Å,[24] thus eliminating the possibility of

Table VI. Nuclear Overhauser Effect Data for Peptides **6** and **7**

resonance		NOE	H---H
irradiated	obsd	(%)	distance[a] (Å)
	Boc-(Acc^6)$_3$-OMe (6)		
Acc^3(1) NH	Acc^6(2) NH	1.9	2.637
	Acc^6(3) NH		4.468
Acc^6(2) NH	Acc^6(1) NH	1.8	2.637
	Acc^6(3) NH	2.5	2.804
Acc^6(3) NH	Acc^6(2) NH	1.2	2.804
	Acc^6(1) NH		4.468
	Boc-Pro-Acc^6-Ala-OMe (7)		
Acc^6 NH	Pro C$^\alpha$H	8.5	2.051
Pro C$^\alpha$H	Acc^6 NH	3.4	2.051

[a] H---H distances are calculated from the hydrogen coordinates in the crystal structures.

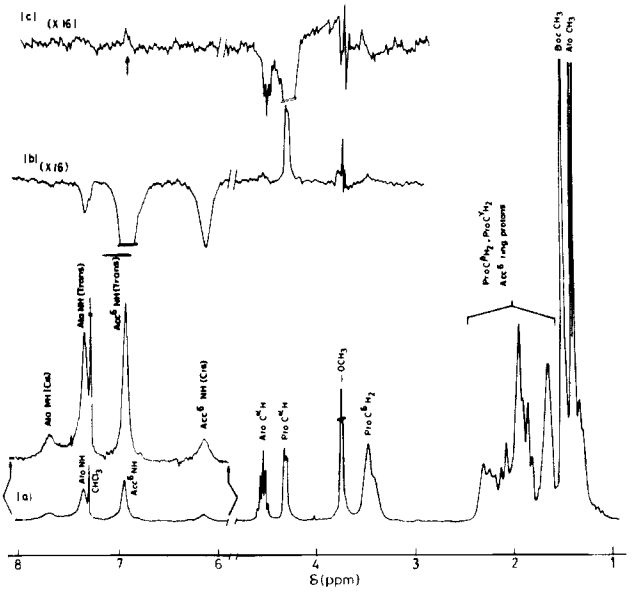

Figure 12. (a) 270-MHz ^{1}H NMR spectrum of Boc-Pro-Acc^6-Ala-OMe (**7**) in $CDCl_3$. Note the presence of lines due to *cis* Boc-Pro conformers. (b and c) Difference NOE spectra obtained by irradiation of (b) Acc^6 NH and (c) Pro C$^\alpha$H resonances. In spectrum b note the transfer of saturation to minor cis conformer resonance. In spectrum c the position of the observed NOE is indicated by an arrow. Vertical scale expansions are indicated. In the NOE experiments 128 accumulations were used. Peptide concentration ~0.05 M.

an NOE between Acc^6(1) NH and Acc^6(3) NH protons. Irradiation of the Acc^6(2) NH resonance results in small enhancements of the Acc^6(1) and Acc^6(3) NH resonances (Figure 11, Table VI). The observation of successive N_iH---$N_{i+1}H$ NOEs is expected in $3_{10}/\alpha$-helical conformations,[24,25] with $\phi_i \sim \phi_{i+1} \sim \pm 50° \pm 20°$ and $\psi_i \sim \psi_{i+1} \sim 40° \pm 20°$. This is consistent with a type III β-turn conformation[19] in **6**, similar to that observed in the solid state. The NH---NH distances determined in the crystal structure (Table VI) are compatible with the NOE data. The magnitudes of the observed NOEs are very small. This is likely to be the case because of alternative relaxation pathways available for NH protons. The estimated NOEs are likely to be subject to considerable error. Nevertheless, in conjunction with hydrogen bonding studies, they provide qualitative support for the retention of the solid-state conformation of **6**, in solution also.

In Boc-Pro-Acc^6-Ala-OMe (**7**) the NMR data summarized in Figure 10 clearly establish that the Ala NH group is strongly solvent shielded, while the Acc^6 NH is fully exposed to solvent. The data then support the involvement of Ala NH in an intra-

(22) (a) Wüthrich, K. *NMR in Biological Research: Peptides and Proteins*; North-Holland: Amsterdam, 1976. (b) Kessler, H. *Angew. Chem., Int. Ed. Engl.* **1982**, *21*, 512–523. (c) Hruby, V. J. *Chemistry and Biochemistry of Amino Acids, Peptides and Proteins*; Weinstein, B., Ed.; Marcel Dekker: New York, 1974; Vol. 3, pp 1–188.

(23) Bothner-By, A. A. *Magnetic Resonance in Biology*; Shulman, R. G., Ed.; Academic Press: New York, 1979; pp 177–219.

(24) Billeter, M.; Braun, W.; Wuthrich, K. *J. Mol. Biol.* **1982**, *155*, 321–346.

(25) Shenderovich, M. D.; Nikiforovich, G. V.; Chipens, G. I. *J. Magn. Reson.* **1984**, *59*, 1-12.

(26) (a) De Tar, D. F.; Luthra, N. *J. Am. Chem. Soc.* **1977**, *99*, 1232–1244. (b) Gratwohl, C.; Wüthrich, K. *Biopolymers* **1976**, *15*, 2025–2041.

molecular hydrogen bond, presumably of the 4→1 type, stabilizing a β-turn conformation. NOE studies in $CDCl_3$ solution serve to establish the nature of the β-turn. Irradiation of the Acc^6 NH resonance results in an NOE of 8.5% on the Pro C$^\alpha$H proton (Figure 12, Table VI), in agreement with a type II β-turn conformation having Pro and Acc^6 at the $i + 1$ and $i + 2$ positions. In the reverse experiment, irradiation of the Pro C$^\alpha$H resonance results in a much smaller NOE of 3–4% on the Acc^6 NH proton (Figure 12), suggesting that alternative relaxation pathways are available to the Acc^6 NH proton. Indeed, for an axial orientation of the amino group in Acc^6, the distances between the NH proton and the axial protons at the two C$^\gamma$ atoms are very short, in most sterically allowed conformations. This should result in appreciable contributions to dipolar relaxation of the NH proton. In the crystal structure of **7**, the observed distances are N(2)H---C(13)H_{ax} = 2.99 Å and N(2)H---C(15)H_{ax} = 2.314 Å. The Acc^6 NH(N-(2)H)---Pro C$^\alpha$H(C(6)H) distance in the crystal is 2.05 Å, compatible with the large NOE observed on the Pro C$^\alpha$H proton, when the Acc^6 NH resonance is irradiated. A notable feature of the NMR spectrum in Figure 12 is the observation of additional resonances in the NH region, assignable to a cis conformation (25%)[27] about the Boc-Pro bond. Appreciable transfer of saturation to the minor resonance at δ 6.11 is seen on irradiating the major Acc^6 NH peak at δ 6.92 (Figure 12b), confirming the assignment of the minor resonance, to a conformation which is in slow exchange with the major species. For cis conformations of the Boc-Pro bond the intramolecular 4→1 hydrogen bond will be broken. The data suggest that the conformation observed in the crystal structure corresponds to the major conformer in $CDCl_3$ solutions of **7**.

Peptides **6** and **7** thus appear to maintain well-defined, folded backbone conformations in solution, similar to those observed in the solid state.

Implications for Conformational Design

The theoretical and experimental results described above establish that Acc^6 residues impart considerable stereochemical rigidity to peptide backbones and are constrained to adopt conformations in the $3_{10}/\alpha$-helical regions of ϕ, ψ space. Acc^6 residues can be accommodated in either position of type III (III′) β-turns or at the $i + 2$ position of type II (II′) β-turns. Considerable recent interest has been focussed on the development of conformationally constrained analogues of biologically active peptides.[27] The availability of highly active, structurally rigid agonists is of value in delineating the nature of receptor bound conformations. Recent studies in this area are exemplified by the development of active *cyclic* analogues of somatostatin,[28] α-melanocyte stimulating hormone,[30] and renin inhibitors.[31] α,α-Dialkylated residues are of particular importance in developing conformationally rigid *acyclic* analogues.[27] Aib containing analogues of enkephalins[32] and chemotactic peptides[33] have been studied. In these studies Gly and Leu residues have been replaced by Aib. Relatively few reports on the use of 1-aminocycloalkanecarboxylic acids (Acc^n) have appeared,[34] but recent studies on chemotactic peptides[7] and aspartame analogues[35] suggest that the greater bulk of the Acc^n side chain ($n \geq 5$) may be of value in binding to hydrophobic pockets at the receptor site. Systematic variations[35] in the size of the Acc^n group can permit an estimation of the size of the binding site for this residue. The backbone conformational restrictions imposed by Acc^6 residues and the similarity of the side chain bulk to that of Val, Leu, and Ile groups suggests that Acc^6 residues should be an important component in the armamentarium of the peptide chemist, in designing stereochemically rigid analogues of biologically active peptides. A comparison of the results obtained in this study for Acc^6, together with earlier reports on α,α-dialkylated residues,[4] clearly establishes that this class of amino acids can be used to stabilize folded, helical structures or fully extended chains, depending on whether cyclic or acyclic substituents are employed.

Acknowledgment. The assistance of S. Raghothama in the NOE experiments is gratefully acknowledged. This research was partially supported by a grant from the Department of Atomic Energy, Government of India.

Registry No. 6, 103732-16-7; **7**, 103732-17-8; Ac-Acc^6-NHMe, 103732-15-6; Ac-Aib-NHMe, 42037-26-3; Ac-Dpg-NHMe, 93039-01-1.

Supplementary Material Available: Tables (S-1–S4, S7, and S8) of bond lengths, bond angles used in obtaining average geometry, anisotropic temperature factors and hydrogen coordinates, and bond lengths and bond angles for crystal structures of Boc-(Acc^6)$_3$-OMe (**6**) and Boc-Pro-Acc^6-Ala-OMe (**7**) (9 pages); tables (S5 and S6) of calculated and observed structure factors for **6** and **7** (22 pages). Ordering information is given on any current masthead page.

(27) (a) Spatola, A. F. *Chemistry and Biochemistry of Amino Acids, Peptides and Proteins*; Weinstein, B., Ed.; Marcel Dekker: New York, 1983; Vol. VII, pp 267–357. (b) Hruby, V. J. *Life Sci.* **1982**, *31*, 189–199.

(28) Veber, D. F.; Freidinger, R. M.; Schwenk-Perlow, D.; Paleveda, W. J., Jr.; Holly, F. W.; Strachan, R. G.; Nutt, R. F.; Arison, B. H.; Homnick, C.; Randall, W. C.; Glitzer, M. S.; Saperstein, R.; Hirschmann, R. *Nature (London)* **1981**, *292*, 55–58.

(29) Schiller, P. W. *The Peptides: Analysis, Synthesis, Biology*; Udenfriend, S., Meienhofer, J., Eds.; Academic Press: New York, 1985; Vol. 7, pp 219–269.

(30) Hadley, M. E.; Anderson, B.; Heward, C. B.; Sawyer, T. K.; Hruby, V. J. *Science* **1981**, *213*, 1025–1027.

(31) Boger, J. *Peptides. Structure and Function*; Hruby, V. J., Rich, D. H., Eds.; Peirce Chemical Co.: Rockford, IL, 1983; pp 569–578.

(32) Sudha, T. S.; Balaram, P. *Int. J. Pept. Protein Res.* **1983**, *21*, 381–388.

(33) Iqbal, M.; Balaram, P.; Showell, H. J.; Freer, R. J.; Becker, E. L. *FEbS Lett.* **1984**, *165*, 171–174.

(34) (a) Tailleur, P.; Berlinguet, L. *Can. J. Chem.* **1962**, *40*, 2214–2217. (b) Park, W. K.; Choi, C.; Rioux, F.; Regoli, D. *Can. J. Chem.* **1974**, *52*, 113–119. (c) Jorgenson, E. C.; Rapaka, S. R.; Windridge, G. C.; Lee, T. C. *J. Med. Chem.* **1971**, *14*, 904–906.

(35) (a) Tsang, J. W.; Schmied, B.; Nyfeler, R.; Goodman, M. *J. Med. Chem.* **1984**, *27*, 1663–1668. (b) Rodriguez, M.; Bland, J. M.; Tsang, J. W.; Goodman, M. *J. Med. Chem.* **1985**, *28*, 1527–1529. (c) Goodman, M. *Biopolymers* **1985**, *24*, 137–155.